Some Placeholder Title

A Master Thesis

written by

Victor Melbye Staven
vista17@student.sdu.dk

The code for this project is available at
`https://github.com/vmstavens/in_hand_pose_estimation`

University of Southern Denmark
The Technical Faculty

Word Count : 962
April 24, 2023

Abstract

Some abstract text explaining the goal, methods and conclusion of the project.

Contents

Acknowledgments . . . ii
Acronyms and Terms . . . iii

1 Introduction **1**
1.1 Context . . . 1
1.2 Problem Description . . . 1
1.3 Thesis Overview . . . 3

2 Modeling **4**

3 State of the Art **8**
3.1 Problem 1 - Tactile Perception . . . 8
3.2 Problem 2 - Pose Estimation . . . 10
3.3 Problem 3 - In-Hand Manipulation . . . 11

4 Tactile Perception **13**
4.1 Introduction . . . 13
4.2 Method . . . 13
4.3 Experimental Setup . . . 13
4.4 Results . . . 13
4.5 Discussion & Conclusion . . . 13

5 Pose Estimation **14**
5.1 Introduction . . . 14
5.2 Related Work . . . 14

6 In-Hand Manipulation **15**
6.1 Introduction . . . 15
6.2 Related Work . . . 15

7 System Integration **16**
7.1 Introduction . . . 16

8 Discussion **17**

9 Conclusion **18**

A Appendix A Title **26**

Acknowledgements

My acknowledgements

Acronyms

AEBM analytical elasticity-based models.
cGAN conditional Generative Adversarial Network.
cobots collaborative robots.
CP correspondence problem.
CPD Coherent Point Drift.
CV computer vision.
DeepGMR Deep Gaussian Mixture Registration.
DL deep learning.
DOF degrees of freedom.
EE end effector.
EFM elastic foundation models.
FEM finite element models.
GK grasp kinematics.
GMM Gaussian Mixture Model.
HF hard finger.
ICP Iterative Closest Point.
IEP Inverse Elasticity Problem.
JRMPC Joint Registration of Multiple Point Sets.
MIM Matrix Inversion Method.
ML machine learning.
MLP Multi Layered Perceptron.
PC point cloud.
PCR point cloud registration.
PE pose estimation.
PNP pick-and-place.
PwoF point-contact-without-friction.
QAP Quadratic Assignment Problem.
RANSAC Random Sample Consensus.
SDP Semi-Definite Programming.
SF soft finger.
SOTA state of the art.

Terms

collaborative robots (cobots) are robots which facilitate human-robot collaboration [1].

computer vision (CV) is a field of artificial intelligence (AI) that enables computers and systems to derive meaningful information from digital images, videos and other visual inputs - and take actions or make recommendations based on that information [2].

correspondence problem (CP) is the problem where one aims at finding correspondences between the pixels in two (or more) images [3].

deep learning (DL) are methods that allow computational models that are composed of multiple processing layers to learn representations of data with multiple levels of abstraction [4].

end effector (EE) is a generic term for all functional units involved in direct interaction of the robot system with the environment or with a given object [5].

manipulator : A serial robot mechanisms. The robot manipulator is represented by a serial chain of rigid bodies, called robot segments, connected by joints [6].

point cloud registration (PCR) is a generic term for all functional units involved in direct interaction of the robot system with the environment or with a given object [5].

pose estimation (PE) A particular instance of feature-based alignment, which occurs very often, is estimating an object's 3D pose from a set of 2D point projections. This pose estimation problem is also known as extrinsic calibration [7].

Chapter 1

Introduction

1.1 Context

As of 2022 most of the industrialized world has developed tools for unprecedented growth in wealth and technology on a global scale [8, Chapter 4]. In such times a great deal of consumerism and interconnection is present with people needing products produced faster and more consistently than ever before [8, Chapter 4]. As one would expect, this creates a high demand for manufacturers to reliably and consistently provide products, while also remaining flexible as the demand for different product change rapidly. To accommodate the need for ever-greater volumes of products, consistent, reliable and flexible labor is essential in assembly, transport and manipulation processes in the production pipeline. Due to these types of manual labor being largely done by unskilled workers, automation alternatives are being adopted which provide benefits [8, Chapter 4]. This different approach to manufacturing has been labeled the fourth industrial revolution or i4.0 for short. The beneficiaries are the employer and employee, with the employer having the benefits: Avoid paying monthly salaries to unskilled laborers doing manual tasks, here the automation alternative only requires electrical energy and potential supervision by a few qualified individuals. Potential risks are also involved when hiring humans as the workforce can be inconsistent due to human error [9] or left out due to illness etc. Considerations about workers' rights such as working conditions and wages also need not be considered. Workers furthermore cause production limitations in the form of stand-still hours, such as bathroom and lunch breaks along with after-work hours and holidays. This replacement of manual labor also potentially benefits the employee, as boring and physically wearing work is automated, enabling the employees to take on different and less wearing and potentially dangerous roles. While the issue of labor unemployment becomes apparent solutions that provide support to already hired workers have been developed, such as collaborative robots (cobots) [10] which would negate this problem.

When implementing automation of production lines using robotics, certain categories of problems are revealed. These include assembly, alteration and pick-and-place (PNP), the last being the one of interest in this project.

1.2 Problem Description

Pick-and-place manipulators are used in a wide variety of different fields such as sorting of waste [11] handling of food [12, 13] and factory bin picking [14, 15, 16]. The solutions in these industries are examples of subcategories under the PNP problem, namely sorting and bin picking. Since both of these are subcategories of the PNP problem, they fundamentally follow the same sequential four phases from start to end. These phases are pre-grasping, grasping, transport, and placement [15] for traditional implementations of the PNP pipeline. The pre-grasp phase involves localizing the object(s), potentially estimating their pose and executing the trajectory to move the end effector (EE) grasp, collision-free to said object(s). Here different potential grasps can be considered to determine the best pose for the EE. In the grasping phase, the EE gasps the object in such a manner that the object's entire weight is supported by the EE, and ends when the object no longer is in contact with the environment, which often is the container holding the object. The transportation phase involves the motion of the manipulator to move from the pose achieved after the grasping phase, to a pose ready for placement of the object in the desired placing area or fixture. Here considerations may be needed about how much force and torque the EE's grasp can tolerate while moving without losing the object. Finally, the goal of the placing phase is to place the object within the placing area or fixture in a desired end pose. Here the constraints on the end pose might differ significantly based on the application, as the pose of greens in a crate might need less precision than if the manipulator hands a bolt to another robotics system in the pipeline.

While these phases make up a traditional PNP system, certain assumptions are made regarding the objects of interest for this pipeline to function. Specifically, the localization and pose estimation (PE) of the pre-grasp phase are assumed possible due to either ensured object poses or estimated poses through computer vision (CV) sensory system. Due to CV being a mature research field a wide range of solution proposals to these problems have been generated [17]. These include classic vision [18, 19], deep learning (DL) based [20] and combinations of these [21]. However, while these may be sufficient for certain tasks they fundamentally suffer from the weaknesses introduced by vision techniques. These are a great number of outliers caused by: occlusions, reflecting, transparent or homogeneous surfaces, and repetitive structures when solving the correspondence problem (CP). Within factory settings, the common ones are transparent and reflective objects, due to metallic, plastic and glass products often being the materials used. While DL solutions have been developed for both reflective [22] and transparent [23] objects, these are use case specific and show limited results in a wider range of applications.

This project suggests a different PNP pipeline for cases where the object's starting pose is unknown. In this PNP pipeline the PE is moved from the pre-grasping phase to a new phase between the grasping and transportation phase, called the PE phase. The specific goal of this project is to develop a solution to this phase using tactile sensors in the EE to determine the object's pose. By using tactile sensing rather than visual the problems presented above will be eliminated. This will be done using a humanoid gripper as the EE with tactile sensors in each finger, more specifically a Shadow Dexterous Hand [24] with 20 degrees of freedom (DOF).

The alternative pipeline this project will enable can be seen in the upper row of Fig. 1.1 compared to the traditional pipeline in the lower row.

In Fig. 1.1(a) the pre-grasping phase can be seen for both pipelines. Here the traditional pipeline in cases of multiple objects often will employ custom fingertips or grippers entirely to facilitate form closure grasps, due to the grippers not having the flexibility to perform reliable force closure. On the contrary force closure can be performed with a humanoid gripper on a wide range of objects with no need for changing gripper equipment.

In Fig. 1.1(b) the grasping phase can be seen which introduces a greater level of complexity when using the suggested pipeline due to the humanoid gripper being a more complex physical system to represent and control. This is compared to the simplicity of executing potential binary commands in the traditional pipeline e.g.open and close.

In Fig. 1.1(c) the transportation phase can be seen, which introduces one of the benefits of using the suggested pipeline. Here tactile sensors in a humanoid gripper can pose and estimate the object and manipulations can be performed to change the object's pose such that easier placement can be performed in the following phase. This form of object manipulation is not feasible for the simple pneumatic grippers used in a traditional pipeline.

In Fig. 1.1(d) the placement phase can be seen, which demonstrates the result of the previous phase, as the traditional pipeline now has to change the grip on the object to properly place it in the socket, while the humanoid gripper simply can insert the part, as it is already oriented properly.

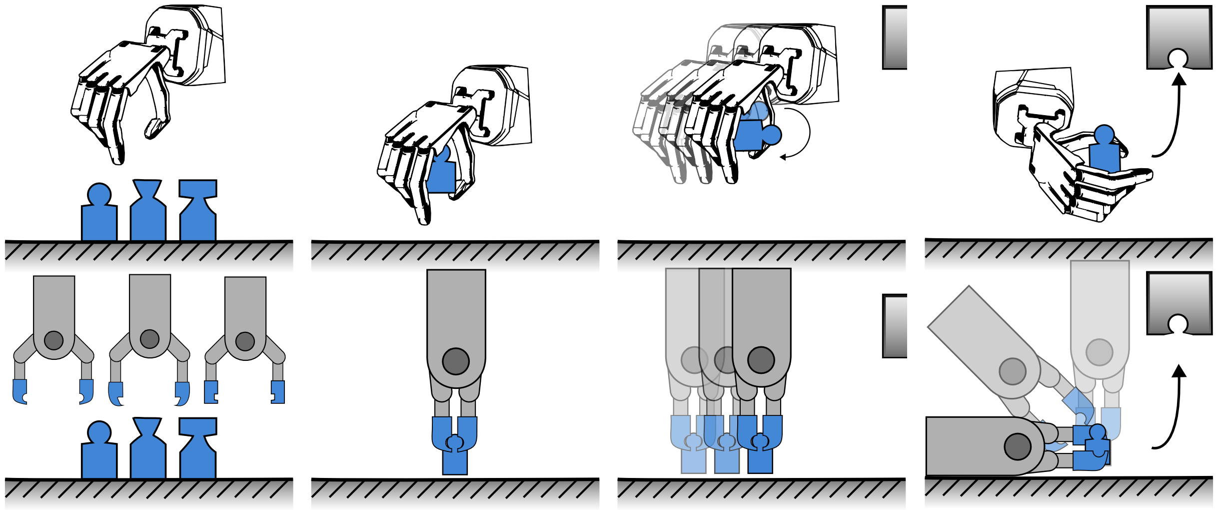

(a) Pre-grasp phase. **(b)** Grasping phase. **(c)** Transportation phase. **(d)** Placement phase.

Fig. 1.1: A comparison between the traditional and suggested PNP pipeline.

To solve this PE problem, three sub-problems are identified and labeled problems 1, 2 and 3.

Problem 1 involves modeling the contact between the gripper's tactile sensors and the object, also referred to as tactile perception.

Problem 2 is to convert the collected data from problem 1 to estimated pose candidates.

Problem 3 involves in-hand manipulation. Since the initial grasp of the object might not be oriented in a manner where the recognizable features make context with the tactile sensors, manipulating the object within the EE's grasp will enable further information gathering. Thus the final problem is to control the EE in such a manner that the tactile sensors make context with the object in intelligently decided areas for a better pose estimate.

To test if the developed system successfully solves the PE problem, it is hypothesized that the intelligent probing method provides a statistically significant faster average PE convergence, along with a statistically significant greater success rate when determining the correct pose. A correct pose is here defined as the pose being greater than or equal to 95 % of the ground truth pose, and statistically significant is defined by an α-level of 95 %. This hypothesis will be referred to as H_1, while the null hypothesis H_0 being that there is no statistically significant difference between intelligent and random probing's PE performance as described above.

1.3 Thesis Overview

To present the work done in this project, the system modeling is done in Chapter 2 and state of the art (SOTA) is presented in Chapter 3 for each of the problems presented above. Here the solutions best suited for this project's gripper are chosen. Each solution is described in detail, how they are applied, their performance tested and finally evaluated and concluded upon in their respective chapters i.e. chapter Chapter 4, Chapter 5 and Chapter 6. In Chapter 7 the three methods are combined in the final integration and finally, the project is discussed and concluded upon in Chapter 8 and Chapter 9 respectively.

Chapter 2

Modeling

To model the contact between the EE's tactile sensors, eight different categories exist as identified in [25]. The three most common ones within the field of robotics [26, Chapter 37] are point-contact-without-friction (PwoF), hard finger (HF) and the soft finger (SF) model as shown in Fig. 2.1.

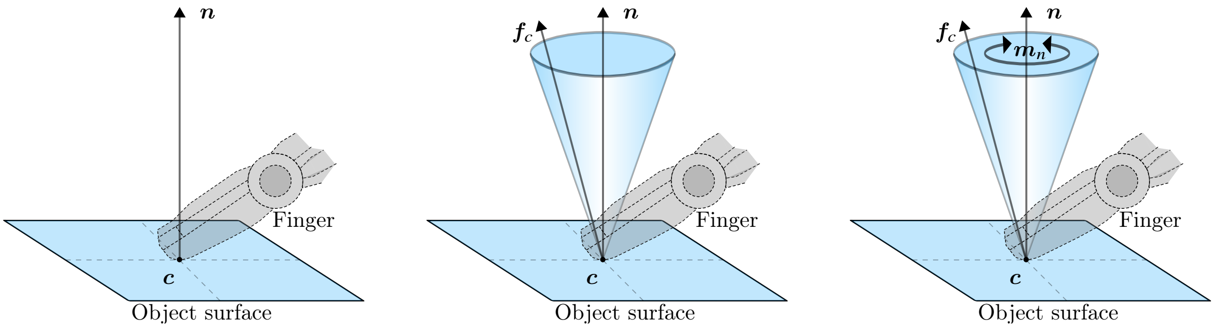

(a) PwoF in point $\boldsymbol{c}$ with normal $\boldsymbol{n}$.

(b) HF in point $\boldsymbol{c}$ with normal $\boldsymbol{n}$ and contact force $\boldsymbol{f}_c$.

(c) SF in point $\boldsymbol{c}$ with normal $\boldsymbol{n}$, contact force $\boldsymbol{f}_c$ and friction moment $\boldsymbol{m}_n$.

Fig. 2.1: The three most commonly used contact models.

The PwoF model, as shown in Fig. 2.1(a), can only represent forces along the surface normal $\boldsymbol{n} \in \mathbb{R}^3$ at the point of contact $\boldsymbol{c} \in \mathbb{R}^3$ and thus the model does not support surface deformations between the two contacting objects. This model is applied in cases where very little deformation is present, along with the contact having a friction coefficient approximately equal to zero [26, Chapter 38].

The HF model, as shown in Fig. 2.1(b), is representative when the friction between objects is significant, while the contact deformation is small enough to ignore friction moments and deformations [26, Chapter 38]. To model the friction acting on the contact point a great number of methods exist, a common one being the Coulomb friction with different modifications depending on the use case [27]. This model states that the frictional force acting on an object can be formulated as

$$f_f = f_N \mu, \tag{2.1}$$

with f_f being the magnitude of the Coulomb friction, f_N being the magnitude of normal force in the point of contact and $\mu \in [0, 1]$ being the friction coefficient. One visualization of this linear relationship can be seen in the cones illustrated in Fig. 2.1(b) and Fig. 2.1(c). These cones are referred to as friction cones, which for a hard finger model can be formulated as

$$C_{f,\mathrm{HF}} = \left\{ f_c \;\middle|\; f_t \leq \mu f_z,\ \mu f_z \geq 0 \right\} \qquad , \qquad f_t = \sqrt{f_x^2 + f_y^2}. \tag{2.2}$$

Here f_c is the magnitude of the contact force, f_t is the magnitude of the tangential force. f_x, f_y and f_z are the magnitudes of the x, y and z components of the contact force ($\boldsymbol{f}_c \in \mathbb{R}^3$) and μ is the friction coefficient [26, Chapter 37]. By applying a contact force that ensures the friction stays greater than the magnitude of the tangential force, neither object slips i.e. f_z must ensure that $f_z\mu$ stays greater than f_t for the objects not to slip. Visually this is the case when the contact force $\boldsymbol{f}_c$ stays within the friction cone, which enables a friction-based grasp type referred to as force closure. Specifically, force closure refers to when the composite wrench cone contains the entire wrench space so that any external wrench $\boldsymbol{w}_{\text{ext}}$ on the body can be balanced by contact forces [28]. A force that commonly contributes significantly to the external wrench, and thus to the tangential force, is gravity.

The SF model, as shown in Fig. 2.1(c), is used to represent scenarios where both friction and surface deformations are significant. Due to deformations of the finger, an additional torsional moment about the contact normal will be present [26, Chapter 38]. While an analytical formulation of the SF relation depends on the pressure distribution inside the contact, and can only be derived for a limited number of special cases, the general case can be approximated using

$$\mathcal{E}_{f,\mathrm{SF}} = \left\{ f_c \;\middle|\; f_t^2 + \frac{m_n^2}{e_n^2} \leq \mu^2 P^2 \right\} \qquad , \qquad f_t = \sqrt{f_x^2 + f_y^2}. \tag{2.3}$$

This formulation forms a contact ellipsoid $\mathcal{E}_{f,\mathrm{SF}}$ which describes the relationship between the tangential force $\boldsymbol{f}_t \in \mathbb{R}^3$ and friction moment $\boldsymbol{m}_n \in \mathbb{R}^3$. The friction parameters in this expression remain the same as for the friction cone, with the additional m_n being the magnitude of the frictional moment, e_n being the eccentricity parameter i.e. the height of the aforementioned ellipsoid and P being the magnitude of the pressure applied from the contact point along the contact normal $\boldsymbol{n}$ [29, 30].

Based on the model categories described above, the most representative for this project's case, are the SF models since these can provide information about the contact surface's shape, thus enabling the reconstruction of the contact shape from the application of a force distribution [31] i.e. the Inverse Elasticity Problem (IEP). Additionally, these models support descriptions of friction which is crucial to manipulate objects in hand. Illustrations of the system as a SF with friction cone, pressure distribution and the enabling of force closure can be seen in Fig. 2.2 and Fig. 2.3 respectively.

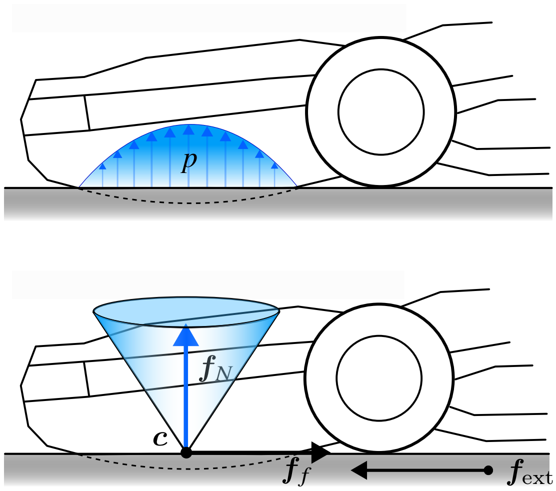

Fig. 2.2: The pressure distribution p and friction cone of a SF model experiencing an external force $\boldsymbol{f}_{\mathrm{ext}}$.

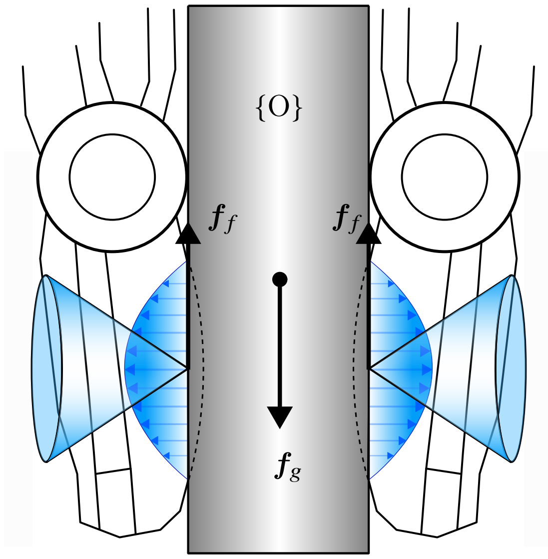

Fig. 2.3: the pressure distribution and friction cone causing force closure to prevent the object {O} from falling due to the gravitational force $\boldsymbol{f}_g$.

When modeling the kinematics of an anthropomorphic gripper with frame $\{\mathrm{H}\} \in \mathbb{R}^{4\times4}$ in world frame $\{\mathrm{W}\} \in \mathbb{R}^{4\times4}$ interacting with an object with frame $\{\mathrm{O}\} \in \mathbb{R}^{4\times4}$ the relevant parameters must be addressed. In this system the object with position $\boldsymbol{p} \in \mathbb{R}^3$ and pose $\boldsymbol{u} \in \mathbb{R}^6$, with the orientation either being represented as a four-dimensional quaternion or a three-dimensional Euler angle, makes contact with the gripper in points $\boldsymbol{c}_i \in \mathbb{R}^3$. These contact points have frames $\{\mathrm{C}\}_i \in \mathbb{R}^{4\times4}$ with axes $\{\boldsymbol{n}_i, \boldsymbol{t}_i, \boldsymbol{o}_i\} \subset \mathbb{R}^3$, where $\boldsymbol{n}_i \in \mathbb{R}^3$ points perpendicular to the contact plain towards the object, while the remaining are contained within the contact plane. For each of these parameters $i = 1, 2, \ldots, n_c$, where n_c is the number of contact points. The twist of {O} described in {W} is denoted $\boldsymbol{\nu} = \left[\boldsymbol{v}^\top \; \boldsymbol{\omega}^\top\right]^\top \in \mathbb{R}^6$ while the non-contact wrench i.e. the wrench caused by external forces such as collisions with the environment and gravity, is $\boldsymbol{w} = \left[\boldsymbol{f}^\top \; \boldsymbol{m}^\top\right]^\top \in \mathbb{R}^6$. The gripper's state is described in terms of its joints, of which it has n_q, named $\boldsymbol{q} = \begin{bmatrix} q_1 \; q_2 \; \cdots \; q_{n_q} \end{bmatrix}^\top \in \mathbb{R}^{n_q}$ each of which is revolute and can exert a torque $\boldsymbol{\tau} = \begin{bmatrix} \tau_1 \; \tau_2 \; \cdots \; \tau_{n_q} \end{bmatrix}^\top \in \mathbb{R}^{n_q}$. These parameters can be seen illustrated in Fig. 2.4 showing the system model. While only a single finger here is illustrated the naming conventions and representations simply scale to all the

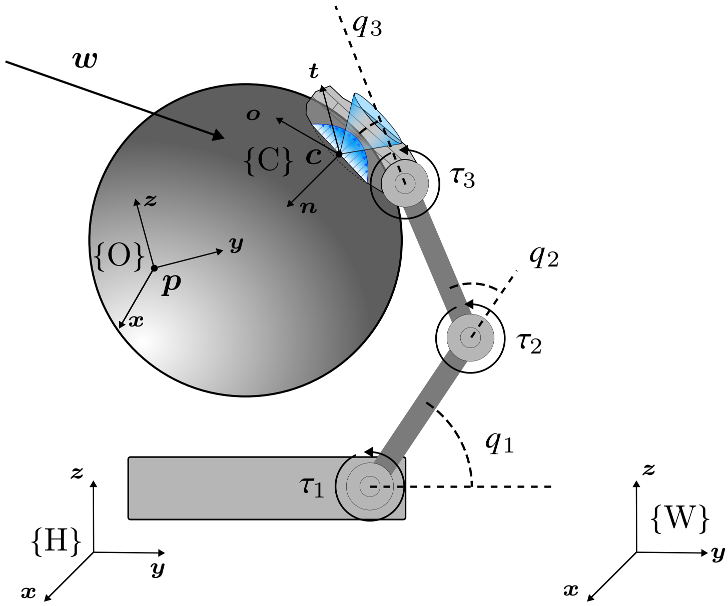

Fig. 2.4: The model of the world representation for this project.

EE's DOFs.

In this system, the twists and wrenches of a contact point $\boldsymbol{c}_i$ on the object and hand, given in contact frame $\{\mathrm{C}\}_i$ is referred to as $\boldsymbol{\nu}_{i,\xi} \in \mathbb{R}^6$ and $\boldsymbol{w}_{i,\xi} \in \mathbb{R}^6$, with $\xi = \{\mathrm{obj}, \mathrm{hnd}\}$. Given multiple contact points, complete vectors of twist and wrench can be expressed by appending each contact point's twist and wrench vector. These contain all twists and wrenches of the grasp, one for the object and one for the hand. These vectors are referred to as

$$\boldsymbol{\nu}_{c,\xi} = \begin{bmatrix} \boldsymbol{\nu}_{1,\xi}^\top \; \boldsymbol{\nu}_{2,\xi}^\top \; \cdots \; \boldsymbol{\nu}_{n_c,\xi}^\top \end{bmatrix}^\top \in \mathbb{R}^{6 \cdot n_c} \tag{2.4}$$

and

$$\boldsymbol{w}_{c,\xi} = \begin{bmatrix} \boldsymbol{w}_{1,\xi}^\top \; \boldsymbol{w}_{2,\xi}^\top \; \cdots \; \boldsymbol{w}_{n_c,\xi}^\top \end{bmatrix}^\top \in \mathbb{R}^{6 \cdot n_c} \tag{2.5}$$

respectively.

These definitions are used to describe and analyze the kinematics of grasping and the parameters involved in holding and manipulating objects in hand, also referred to as grasp kinematics (GK). Within GK two matrices are of special interest: the grasping matrix $\mathbf{G}$ and the hand Jacobian $\mathbf{J}$. The grasping matrix describes the transformation between the twist or wrench of the object in world frame $\{\mathrm{W}\}$ to the twists or wrenches of the object in contact frames $\{\mathrm{C}\}_i$. The grasp matrix thus can be expressed as

$$\mathbf{G} = \begin{bmatrix} \mathbf{G}_1 \; \mathbf{G}_2 \; \mathbf{G}_3 \; \cdots \; \mathbf{G}_{n_c} \end{bmatrix}, \tag{2.6}$$

where $\mathbf{G}_i \in \mathbb{R}^{6\times6}$ describes the transformation from $\{\mathrm{W}\}$ to the individual $\{\mathrm{C}\}_i$, and thus $\mathbf{G} \in \mathbb{R}^{6\times6\cdot n_c}$ describes the transformations for all contact points. Using this grasp matrix, the object wrench and twist can be computed in all contact frames as

$$\boldsymbol{\nu}_{c,\mathrm{obj}} = \mathbf{G}^\top \boldsymbol{\nu} \qquad \text{and} \qquad \boldsymbol{w}_{c,\mathrm{obj}} = \mathbf{G}^\top \boldsymbol{w}. \tag{2.7}$$

While the grasp matrix describes the transformation from $\{\mathrm{W}\}$ to object contact frames, the hand Jacobian relates the joint velocities and torques to the contact twists and wrenches on the hand. The hand Jacobian can thus be expressed as

$$\mathbf{J} = \left[\mathbf{J}_1^\top \; \mathbf{J}_2^\top \; \mathbf{J}_3^\top \; \cdots \; \mathbf{J}_{n_c}^\top\right]^\top, \tag{2.8}$$

for all contact points. Here $\mathbf{J}_i \in \mathbb{R}^{6 \times n_q}$ for $i = 1, 2, \ldots, n_c$ are the individual contact point's hand Jacobians and thus $\mathbf{J} \in \mathbb{R}^{6 \cdot n_c \times n_q}$ is the complete. Using the complete hand Jacobian, the contact twists and wrenches on the hand can be related to the joint velocities and torques as

$$\boldsymbol{\nu}_{c,\mathrm{hnd}} = \mathbf{J}\dot{\boldsymbol{q}} \qquad \text{and} \qquad \boldsymbol{\tau} = \mathbf{J}^\top \boldsymbol{w}_{c,\mathrm{hnd}}. \tag{2.9}$$

The modeling described above will enable the use of methods for solving the presented problems. These methods will be determined in Chapter 3.

Chapter 3

State of the Art

3.1 Problem 1 - Tactile Perception

Based on the contact model categories described in Chapter 2, the most representative was chosen to be SF models. Within the category of SF models, a method fit for this project's use case is to be chosen to solve problem 1. SF models can furthermore be divided up into three different categories: analytical elasticity-based models (AEBM), elastic foundation models (EFM), finite element models (FEM) [32] and machine learning (ML) models. The different categories can be seen organized in Fig. 3.1

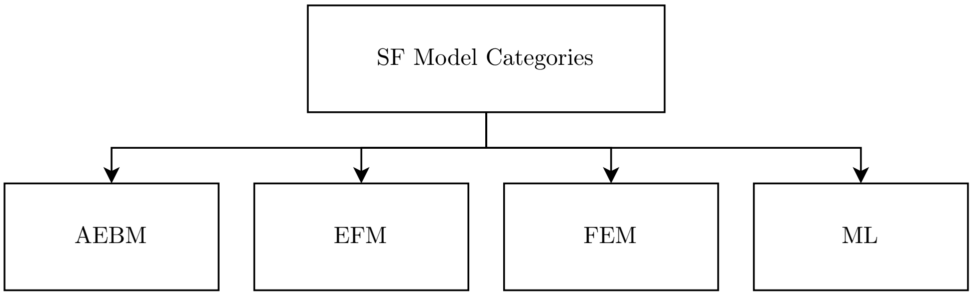

Fig. 3.1: Tree of methods for tactile perception.

AEBM are theoretical formulations of elastic contact areas and the stresses on both the surfaces and the sub-surfaces of the contacting bodies. The first of such models was introduced by Heinrich Rudolf Hertz in 1882 [33] and is still used for simple contact cases. In the formulation of the Hertzian contact model, two assumptions are made: Objects in contact are made of linear elastic materials and only small contact deformations occur compared to the dimension of an object. However, robotic EE fingertips are often made of non-linear elastic materials and for that reason, the Hertzian contact model does not represent the type of contact in this project [26, Chapter 37]. To improve on the Hertzian model, a more general formulation can be made which extends the model from linear to nonlinear elastic contacts [34, 35]. This power-law formulation subsumes the Hertzian contact theory while assuming a circular contact area. Other models have been purposed that combine the descriptions of both friction-contact and the shear-torsion as experienced by the bodies [36].

However, to more accurately describe the contacts involving robot fingers, viscoelastic soft contact model appear more relevant due to such fingers often being made of materials that show viscoelastic properties e.g., rubber, silicone and polymers. Simple models such as Kelvin-Voigt's [37] and Maxwell's [38] models describe the interaction between strain and stress as a spring-damper system in a serial or in a parallel configuration respectively. Models which expand on this idea describe the reacting force as the product of the temporal and the elastic response while incorporating previous stress responses [39]. To simplify this formulation alternatives have been developed to assume no past stress [40, 41, 42]. Upon these, more modern techniques have been developed which have seen use in similar use cases as the ones of interest in this project. One method attempts to expand the description of contacts between rigid indentors and elastic half-spaces, using the Matrix Inversion Method (MIM) as introduced by Kalker [43], to viscoelastic half-spaces as well. Assuming the surfaces are frictionless, the relationship is described in terms of the pressure distribution, the resultant force on the indenter and the penetration [44]. Attempts involving solutions to Boussinesq's problem for polynomial pressures acting over polygonal domains [45] have also been developed and modernized by combining it with Cerruti's solution [46]. However due to numerical singularities being present, modifications are made to threshold the model. For a more complete description without singularities, Love's formulation has been added leading to a more accurate analytical representation but with the cost of an increased computational complexity [47]. For these Boussinesq-based approaches to be representative two assumptions are made 1) There exists a linear relationship between stress and strain, referred to as deformation, and 2) strains are infinitesimal [48, Chapter 6].

EFM are methods developed to build upon AEBM by allowing a simple discrete contact calculation in more general surface geometries. Here the deformable part of the contact is modeled as a layer over a rigid base with a series of discrete and independent springs in the contact normal. A widely used example of this method is Winkler's elastic foundation model [49], which has been used in structural engineering for modeling different properties of beams such as stability [50], vibrations and buckling [51]. Other EFM methods have shown accurate modeling performance when applied within the field of medical engineering. Here a comparative study between AEBM, EFM and FEM demonstrate the suggested modified EFM performs better than the alternatives in 3D knee models when predicting prosthetic knee performance [32]. A different method attempts to attain vivo contact pressure predictions for improved knee replacement designs [52] Within the field of robotics EFM have provided solutions to problems such as slip [36], compliance, sliding [53, 29], stiffness and contact mechanics [54] of anthropomorphic grippers. One such method derives friction constraints based on general expressions for non-planar contacts of elastic bodies, where the local geometry and structure of the objects in contact are taken into account. Using these, a linear complementary problem is formulated and solved, resulting in the normal and frictional forces applied at each contact, as well as the relative velocity of the bodies involved [30].

FEM are popular general tools for solving PDE [55] and have seen contact applications in a wide range of engineering disciplines due to the assumptions made in AEBM and EFM not being applicable in these cases. A great number of these cases exist within the manufacturing industry [56] whereas one example is the metal forming processes. Specifically, the estimation of wheel-rail profiles [57] has been addressed using FEM due to the estimation of contacts over a greater surface is needed than what is assumed in AEBM and EFM. Other applications such as quality control through sliding wear estimation [58], analysis of the responses of fully coupled thermo-elasto-plastic solids in contact [59] and performing diagnostics of failures in induction motors [60]. Due to the complexity of modeling the contacts within robotics, FEM have become a popular choice and enabled tactile applications such as cobots tactile skin for ensuring collaborative behavior when in contact [61], performance estimation of new tactile sensor technologies [62] and evaluating complex contact types by extending simulations and analysis systems [63]. The modeling complexity has furthermore inspired using FEM as ground truth results when synthesizing ML data in simulations for deep learning models, which has enabled execution speeds 75 times greater than simply evaluating FEM [64, 65, 66].

The use of these ML models has enabled realistic simulations of tactile sensor data. Current literature applies DL-based approaches to simulate tactile sensor data for various tasks [67, 68]. For instance, simulating realistic tactile images from simulated contact depth to bridging the reality gap for vision-based tactile sensing using a diffusion model [69]. Similarly, a conditional Generative Adversarial Network (cGAN) has been used to simulate realistic tactile sensory data for use in tactile tasks [69]. Solutions using simple Multi Layered Perceptron (MLP) have been applied to enable real-time simulated realistic tactile data [70].

Given the methods presented above, the AEBM Boussinesq-Cerruti approach is considered along with the ML approach with a MLP model.

Although the Boussinesq-Cerruti approach can produce precise tactile data and can be tailored to suit a particular case, it faces certain challenges. The model relies on certain assumptions regarding the materials in contact, including linear deformation and infinitesimal strains. Furthermore, evaluating the model requires complex calculations, such as multidimensional integrals, which significantly increase computation time and hinder real-time performance. In contrast to the transparency offered by the Boussinesq-Cerruti approach, the MLP approach is limited by the black-box nature of DL models. Despite this drawback, MLPs offer several benefits, such as low execution time and high adaptability to complex systems. Due to the high adaptability and option for real-time performance, the MLP model presented in [70] is chosen to solve the tactile perception problem i.e. problem 1.

3.2 Problem 2 - Pose Estimation

PE, which involves determining the position and orientation of an object in 3D space, has been the subject of many research studies. The literature has identified two main categories of methods for solving this problem: those based on DL, and those based on point cloud registration.

These can along with their subcategories be seen in Fig. 3.2 as inspired by [71].

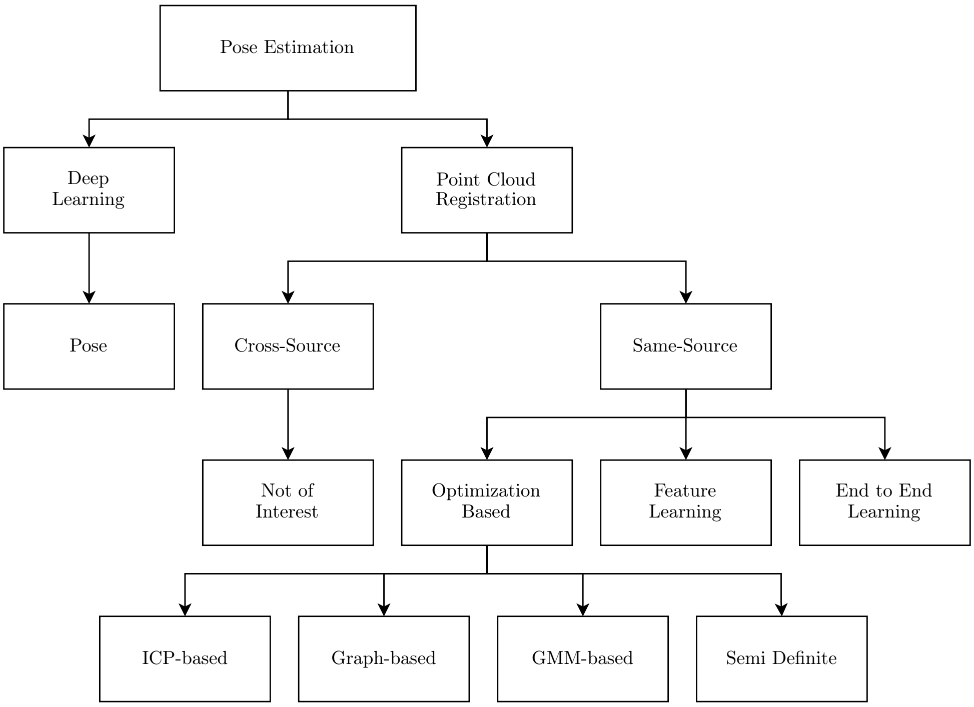

Fig. 3.2: Tree of methods for solving the point cloud registration problem. The categorization is inspired by [71].

Purely DL based methods learn feature representations of input data, often in the form of images, and use them to estimate the subject's pose. This is commonly done in the context of human pose estimation [72, 73, 74]. While these methods have shown extensive use in these cases, their applicability in this project is limited and thus excluded from consideration.

The other method group i.e. point cloud registration (PCR) methods are separated into two subgroups: cross-source and same-source point cloud (PC)s. Here cross-source refers to a PC produced by combining information from sensors of different kinds e.g. visual- and tactile sensors, while same-source methods only produce PCs based on information from the same kind of sensors e.g. only tactile sensors. While cross-source approaches have shown utility in an extensive range of applications [75, 76, 71] their applicability in this project is minimal, as purely tactile pose estimation is the problem of interest as presented in Chapter 1.

PCR methods from the same source data can be categorized into three sub-categories: end-to-end learning, feature-learning, and optimization-based methods. End-to-end learning-based methods use a neural network to estimate the transformation matrix that aligns two point clouds. Proposed solutions include using neural networks for scene completion to estimate the relative pose between RGB-D scans [77], learning registration patterns as parametric functions through a scan completion module and pairwise matching module [78], and a fast feature-metric point cloud registration framework to minimize the feature-metric projection error without correspondences [79].

In contrast, feature-learning methods use deep neural networks to learn robust feature correspondence searches, which are then used in estimation algorithms such as Random Sample Consensus (RANSAC). In the literature, models have been developed to extract local geometric descriptors from RGB-D reconstructions [80], to learn globally informed 3D local feature descriptors [81], and to use siamese deep learning architectures with convolutional layers through a voxelized smoothed density value (SDV) representation [82].

Lastly, registration methods based on optimization are employed to estimate the transformation matrix through two stages: correspondence searching and transformation estimation. Their goal is to minimize a cost function that gauges the dissimilarity between two point clouds. Within this category, there are four sub-categories identified: Iterative Closest Point (ICP)-based, graph-based, Gaussian Mixture Model (GMM)-based, and semi-definite programming-based methods.

Since the original proposal in 1992 [83] using point-to-point correspondences, ICP-based methods have evolved and incorporated different types of correspondences to improve performance. Examples include point-to-plane [84] and plane-to-plane [85]. Modern approaches also employ complementary methods such as point cloud filtering, adaptive fireworks algorithms, and KD-Trees [86].

The main idea of graph-based registration methods is to use a non-parametric model [87]. In this method, correspondences between two graphs are found by considering both the vertices and edges, making it an optimization problem [87]. To solve this optimization problem, there are two categories of graph-matching methods based on the objective functions' constraints: second-order and high-order methods [88].Second-order methods include CSGM [75], which uses a linear program to solve the graph-matching problem and apply it to solve the cross-source point cloud registration task, FGM [89] factorizes the large pairwise affinity matrix into smaller matrices and solves the graph-matching problem with a simple path-following optimization algorithm. Spectral graph [90] uses a spectral relaxation method to approximate the Quadratic Assignment Problem (QAP), and Semi-Definite Programming (SDP) relaxation is used to relax the non-convex constraint using a convex semi-definite. While higher-order graph matching provide method for [91] design a probabilistic approach to solve the high-order graph-matching problem, while [92] design a triangle similarity and convert the graph-matching problem into a tensor optimization problem. More recent work, such as [93] suggests an elastic net to control the trade-off between the sparsity and accuracy of the matching results by incorporating the Elastic-Net constraint into the tensor-based graph matching mode.

GMM-based methods commonly tackle the point cloud registration problem by transforming it into a likelihood maximization problem for the input data. This has resulted in the development of several optimization strategies aimed at maximizing the likelihood and optimizing the transformation matrix. For instance, a motion drift idea was introduced into the GMM framework by [94] in the form of Coherent Point Drift (CPD) which imposes constraints on transformation estimation. In another approach,[95] combines GMM with the convex hull to reduce computation complexity. Furthermore, Joint Registration of Multiple Point Sets (JRMPC) [96] cast registration as a clustering problem where the transformation is optimized by solving the GMM. Recently, Deep Gaussian Mixture Registration (DeepGMR) [97] employed DL to learn the correspondences between GMM components and points, enabling the estimation of both the transformation and GMM parameters in a single forward step.

Lastly

3.3 Problem 3 - In-Hand Manipulation

References:

resources:

Chapter 4

Tactile Perception

4.1 Introduction

- start with performance specifications regarding the two problems the tactile perception should be able to solve: can the are the points representative, according to the source yes, but are the normals also representative. This is important for the pose estimation problem. When manipulating the object the finger needs to be able to exert enough friction to be able to hold the object, is this true. compute the contact friction and see if it is stronger than the gravity on the subject. Use numbers to verify if the performance is acceptable
-

4.2 Method

4.3 Experimental Setup

4.4 Results

4.5 Discussion & Conclusion

Chapter 5

Pose Estimation

5.1 Introduction

Here we write the introduction for problem 2.

5.2 Related Work

Chapter 6

In-Hand Manipulation

6.1 Introduction

Here we write the introduction for problem 3.

6.2 Related Work

For history see hand book of robotics chapter 38, the first section.

Chapter 7

System Integration

7.1 Introduction

Here we write the introduction for the system integration.

Chapter 8

Discussion

Chapter 9

Conclusion

Bibliography

[1] El Zaatari, Shirine et al. "Cobot programming for collaborative industrial tasks: An overview". In: *Robotics and Autonomous Systems* 116 (June 2019), pp. 162–180. DOI: 10.1016/j.robot.2019.03.003.

[2] *What is computer vision?* https://www.ibm.com/topics/computer-vision. Accessed: 2022-11-02.

[3] Zimmer, Henning. "Correspondence problems in computer vision". PhD thesis. Jan. 2012.

[4] LeCun, Yann, Bengio, Yoshua, and Hinton, Geoffrey. "Deep learning". In: *Nature* 521.7553 (May 2015), pp. 436–444. ISSN: 1476-4687. DOI: 10.1038/nature14539. URL: https://doi.org/10.1038/nature14539.

[5] Monkman, Gareth J. et al. "Robot Grippers". PhD thesis. Jan. 2004, pp. 5–6.

[6] Mihelj, Matjaž et al. "Robotics Second Edition". PhD thesis. Jan. 2019, p. 1.

[7] Szeliski, Richard. *Computer vision: algorithms and applications*. Springer Nature, 2022, p. 284.

[8] Publications, United Nations. "Inequality in Asia and the Pacific in the Era of the 2030 Agenda for Sustainable Development". In: 7May 2018. URL: https://www.unescap.org/publications/inequality-asia-and-pacific-era-2030-agenda-sustainable-development.

[9] Wenwen, Shi et al. "Analysis and Control of Human Error". In: *Procedia Engineering* 26 (Dec. 2011), pp. 2126–2132. DOI: 10.1016/j.proeng.2011.11.2415.

[10] Galin, Rinat et al. "Cobots and the benefits of their implementation in intelligent manufacturing". In: *IOP Conference Series: Materials Science and Engineering* 862 (May 2020), p. 032075. DOI: 10.1088/1757-899X/862/3/032075.

[11] Raptopoulos, Fredy, Koskinopoulou, Maria, and Maniadakis, Michail. "Robotic Pick-and-Toss Facilitates Urban Waste Sorting". In: *2020 IEEE 16th International Conference on Automation Science and Engineering (CASE)*. 2020, pp. 1149–1154. DOI: 10.1109/CASE48305.2020.9216746.

[12] Talpur, Mir Sajjad Hussain and Shaikh, Murtaza Hussain. *Automation of Mobile Pick and Place Robotic System for Small Food Industry*. 2012. DOI: 10.48550/ARXIV.1203.4475. URL: https://arxiv.org/abs/1203.4475.

[13] Yamanaka, Yuta et al. "Development of a Food Handling Soft Robot Hand Considering a High-speed Pick-and-place Task". In: *2020 IEEE/SICE International Symposium on System Integration (SII)*. 2020, pp. 87–92. DOI: 10.1109/SII46433.2020.9026282.

[14] Lee, Sukhan and Lee, Yeonho. "Real-Time Industrial Bin-Picking with a Hybrid Deep Learning-Engineering Approach". In: *2020 IEEE International Conference on Big Data and Smart Computing (BigComp)*. 2020, pp. 584–588. DOI: 10.1109/BigComp48618.2020.00015.

[15] Mnyusiwalla, Hussein et al. "A Bin-Picking Benchmark for Systematic Evaluation of Robotic Pick-and-Place Systems". In: *IEEE Robotics and Automation Letters* 5.2 (2020), pp. 1389–1396. DOI: 10.1109/LRA.2020.2965076.

[16] Wong, Ching-Chang et al. "Generic Development of Bin Pick-and-Place System Based on Robot Operating System". In: *IEEE Access* 10 (2022), pp. 65257–65270. DOI: 10.1109/ACCESS.2022.3182114.

[17] He, Zaixing et al. "6D Pose Estimation of Objects: Recent Technologies and Challenges". In: *Applied Sciences* 11.1 (2021). ISSN: 2076-3417. DOI: 10.3390/app11010228. URL: https://www.mdpi.com/2076-3417/11/1/228.

[18] ., Taryudi and Wang, Ming-Shyan. "3D object pose estimation using stereo vision for object manipulation system". In: May 2017, pp. 1532–1535. DOI: 10.1109/ICASI.2017.7988217.

[19] Oh, Jong-Kyu, Lee, Sukhan, and Lee, Chan-Ho. "Stereo vision based automation for a bin-picking solution". In: *International Journal of Control, Automation and Systems* 10.2 (Apr. 2012), pp. 362–373. ISSN: 2005-4092. DOI: 10.1007/s12555-012-0216-9. URL: https://doi.org/10.1007/s12555-012-0216-9.

[20] Abdelaal, Mahmoud et al. "Uncalibrated stereo vision with deep learning for 6-DOF pose estimation for a robot arm system". In: *Robotics and Autonomous Systems* 145 (2021), p. 103847. ISSN: 0921-8890. DOI: https://doi.org/10.1016/j.robot.2021.103847. URL: https://www.sciencedirect.com/science/article/pii/S0921889021001329.

[21] Nakano, Yoshihiro. "Stereo Vision Based Single-Shot 6D Object Pose Estimation for Bin-Picking by a Robot Manipulator". In: *CoRR* abs/2005.13759 (2020). arXiv: 2005.13759. URL: https://arxiv.org/abs/2005.13759.

[22] Kozák, Viktor et al. "Data-Driven Object Pose Estimation in a Practical Bin-Picking Application". In: *Sensors* 21.18 (2021). ISSN: 1424-8220. DOI: 10.3390/s21186093. URL: https://www.mdpi.com/1424-8220/21/18/6093.

[23] Xu, Chi et al. "6DoF Pose Estimation of Transparent Object from a Single RGB-D Image". In: *Sensors* 20.23 (2020). ISSN: 1424-8220. DOI: 10.3390/s20236790. URL: https://www.mdpi.com/1424-8220/20/23/6790.

[24] Straszheim, Troy et al. *Shadow Robot*. URL: https://www.shadowrobot.com/dexterous-hand-series/. (accessed: 29.07.2022).

[25] Salisbury, J. Kenneth and Craig, John J. "Articulated Hands: Force Control and Kinematic Issues". In: *The International Journal of Robotics Research* 1.1 (1982), pp. 4–17. DOI: 10.1177/027836498200100102. eprint: https://doi.org/10.1177/027836498200100102. URL: https://doi.org/10.1177/027836498200100102.

[26] Bruno Siciliano, Oussama Khatib, ed. *Springer Handbook of Robotics*. Springer Berlin, Heidelberg, 2016.

[27] Jonker, Ben, Waiboer, Rob, and Aarts, Ronald. "Modelling of joint friction in robotic manipulators with gear transmissions". In: Jan. 2007, pp. 221–243. ISBN: 10-1-4020-5683-4.

[28] Lynch, Kevin M and Park, Frank C. *Modern Robotics: Mechanics, Planning, and Control*. English (US). Cambridge Univeristy Press, 2017. ISBN: 978-1107156302.

[29] Howe, Robert D. and Cutkosky, Mark R. "Practical Force-Motion Models for Sliding Manipulation". In: *The International Journal of Robotics Research* 15.6 (1996), pp. 557–572. DOI: 10.1177/027836499601500603. eprint: https://doi.org/10.1177/027836499601500603. URL: https://doi.org/10.1177/027836499601500603.

[30] Ciocarlie, Matei, Lackner, Claire, and Allen, Peter. "Soft Finger Model with Adaptive Contact Geometry for Grasping and Manipulation Tasks". In: *Second Joint EuroHaptics Conference and Symposium on Haptic Interfaces for Virtual Environment and Teleoperator Systems (WHC'07)*. 2007, pp. 219–224. DOI: 10.1109/WHC.2007.103.

[31] Ghaednia, Hamed et al. "Contact Mechanics". In: Nov. 2013, pp. 93–140. ISBN: 978-1-4614-1944-0. DOI: 10.1007/978-1-4614-1945-7_3.

[32] Pérez-González, Antonio et al. "A modified elastic foundation contact model for application in 3D models of the prosthetic knee". In: *Medical Engineering & Physics* 30.3 (2008), pp. 387–398. ISSN: 1350-4533. DOI: https://doi.org/10.1016/j.medengphy.2007.04.001. URL: https://www.sciencedirect.com/science/article/pii/S1350453307000616.

[33] Hertz, H. “On the Contact of Rigid Elastic Solids and on Hardness”. In: *Ch 6: Assorted Papers* (1882).

[34] Xydas, Nicholas and Kao, Imin. “Modeling of Contact Mechanics and Friction Limit Surfaces for Soft Fingers in Robotics, with Experimental Results”. In: *The International Journal of Robotics Research* 18.9 (1999), pp. 941–950. DOI: 10.1177/02783649922066673. eprint: https://doi.org/10.1177/02783649922066673. URL: https://doi.org/10.1177/02783649922066673.

[35] Yuvaraj, S., Malayalamurthi, R., and Raja, K. Venkatesh. “The haptic and perceptional characteristics of an anthropomorphic curved soft finger structure”. In: *Curved and Layered Structures* 6.1 (2019), pp. 161–168. DOI: doi:10.1515/cls-2019-0013. URL: https://doi.org/10.1515/cls-2019-0013.

[36] Howe, R.D., Kao, I., and Cutkosky, M.R. “The sliding of robot fingers under combined torsion and shear loading”. In: *Proceedings. 1988 IEEE International Conference on Robotics and Automation*. 1988, 103–105 vol.1. DOI: 10.1109/ROBOT.1988.12032.

[37] Flugge, Wilhelm. *Viscoelasticity*. Blaisdell Publishing Company, Waltham, MA, 1967.

[38] Maxwell, James Clerk. *On the dynamical theory of gases*. Royal Society, 1January 1867.

[39] Fung, Yuan-Cheng. “Mechanical properties and active remodeling of blood vessels”. In: *Biomechanics*. Springer, 1993.

[40] Tiezzi, Paolo and Kao, Imin. “Modeling of Viscoelastic Contacts and Evolution of Limit Surface for Robotic Contact Interface”. In: *Robotics, IEEE Transactions on* 23 (May 2007), pp. 206–217. DOI: 10.1109/TRO.2006.889494.

[41] Tiezzi, P. and Kao, I. “Characteristics of contact and limit surface for viscoelastic fingers”. In: *Proceedings 2006 IEEE International Conference on Robotics and Automation, 2006. ICRA 2006.* 2006, pp. 1365–1370. DOI: 10.1109/ROBOT.2006.1641899.

[42] Tiezzi, Paolo, Kao, Imin, and Vassura, G. “Effect of layer compliance on frictional behavior of soft robotic fingers”. In: *Advanced Robotics* 21 (Oct. 2007), pp. 1653–1670. DOI: 10.1163/156855307782227390.

[43] Kalker, J. J. “On the Contact Problem in Elastostatics”. In: *Unilateral Problems in Structural Analysis*. Ed. by Del Piero, Gianpietro and Maceri, Franco. Vienna: Springer Vienna, 1985, pp. 81–85. ISBN: 978-3-7091-2632-.

[44] Kozhevnikov, I.F. et al. “A new algorithm for computing the indentation of a rigid body of arbitrary shape on a viscoelastic half-space”. In: *International Journal of Mechanical Sciences* 50.7 (2008), pp. 1194–1202. ISSN: 0020-7403. DOI: https://doi.org/10.1016/j.ijmecsci.2008.04.003. URL: https://www.sciencedirect.com/science/article/pii/S0020740308000623.

[45] Marmo, Francesco and Rosati, Luciano. “A General Approach to the Solution of Boussinesq’s Problem for Polynomial Pressures Acting over Polygonal Domains”. In: *Journal of Elasticity* 122.1 (Jan. 2016), pp. 75–112. ISSN: 1573-2681. DOI: 10.1007/s10659-015-9534-5. URL: https://doi.org/10.1007/s10659-015-9534-5.

[46] Li, Junshan and Berger, Edward J. “A Boussinesq–Cerruti Solution Set for Constant and Linear Distribution of Normal and Tangential Load over a Triangular Area”. In: *Journal of elasticity and the physical science of solids* 63.2 (May 2001), pp. 137–151. ISSN: 1573-2681. DOI: 10.1023/A:1014013425423. URL: https://doi.org/10.1023/A:1014013425423.

[47] Wasko, Wojciech et al. “Contact Modelling and Tactile Data Processing for Robot Skins”. In: *Sensors* 19.4 (2019). ISSN: 1424-8220. DOI: 10.3390/s19040814. URL: https://www.mdpi.com/1424-8220/19/4/814.

[48] Slaughter, William S. *The Linearized Theory of Elasticity*. Springer, 2012.

[49] Hills, D., Nowell, D., and Barber, James. “KL Johnson and contact mechanics”. In: *Proceedings of the Institution of Mechanical Engineers, Part C: Journal of Mechanical Engineering Science* 231 (Feb. 2016). DOI: 10.1177/0954406216634121.

[50] Lee, S.Y., Kuo, Y.H., and Lin, F.Y. “Stability of a Timoshenko beam resting on a Winkler elastic foundation”. In: *Journal of Sound and Vibration* 153.2 (1992), pp. 193–202. ISSN: 0022-460X. DOI: https://doi.org/10.1016/S0022-460X(05)80001-X. URL: https://www.sciencedirect.com/science/article/pii/S0022460X0580001X.

[51] Eisenberger, M. and Clastornik, J. “Vibrations and buckling of a beam on a variable winkler elastic foundation”. In: *Journal of Sound and Vibration* 115.2 (1987), pp. 233–241. ISSN: 0022-460X. DOI: https://doi.org/10.1016/0022-460X(87)90469-X. URL: https://www.sciencedirect.com/science/article/pii/0022460X8790469X.

[52] Fregly, Benjamin J., Bei, Yanhong, and Sylvester, Mark E. “Experimental evaluation of an elastic foundation model to predict contact pressures in knee replacements”. In: *Journal of Biomechanics* 36.11 (2003), pp. 1659–1668. ISSN: 0021-9290. DOI: https://doi.org/10.1016/S0021-9290(03)00176-3. URL: https://www.sciencedirect.com/science/article/pii/S0021929003001763.

[53] Kao, Imin and Cutkosky, Mark R. “Quasistatic Manipulation with Compliance and Sliding”. In: *The International Journal of Robotics Research* 11.1 (1992), pp. 20–40. DOI: 10.1177/027836499201100102. eprint: https://doi.org/10.1177/027836499201100102. URL: https://doi.org/10.1177/027836499201100102.

[54] Kao, Imin and Yang, Fuqian. “Stiffness and Contact Mechanics for Soft Fingers in Grasping and Manipulation”. In: *Robotics and Automation, IEEE Transactions on* 20 (Mar. 2004), pp. 132–135. DOI: 10.1109/TRA.2003.820868.

[55] Sabat, Lovely and Kundu, Chinmay Kumar. “History of Finite Element Method: A Review”. In: *Recent Developments in Sustainable Infrastructure*. Ed. by Das, Bibhuti Bhusan et al. Singapore: Springer Singapore, 2021, pp. 395–404. ISBN: 978-981-15-4577-1.

[56] Klocke, Fritz et al. “Examples of FEM application in manufacturing technology”. In: *Journal of Materials Processing Technology* 120.1 (2002), pp. 450–457. ISSN: 0924-0136. DOI: https://doi.org/10.1016/S0924-0136(01)01210-9. URL: https://www.sciencedirect.com/science/article/pii/S0924013601012109.

[57] Telliskivi, T and Olofsson, U. “Contact mechanics analysis of measured wheel-rail profiles using the finite element method”. In: *Proceedings of the Institution of Mechanical Engineers, Part F: Journal of Rail and Rapid Transit* 215.2 (2001), pp. 65–72. DOI: 10.1243/0954409011531404. eprint: https://doi.org/10.1243/0954409011531404. URL: https://doi.org/10.1243/0954409011531404.

[58] Põdra, Priit and Andersson, Sören. “Simulating sliding wear with finite element method”. In: *Tribology International* 32.2 (1999), pp. 71–81. ISSN: 0301-679X. DOI: https://doi.org/10.1016/S0301-679X(99)00012-2. URL: https://www.sciencedirect.com/science/article/pii/S0301679X99000122.

[59] Pantuso, Daniel, Bathe, Klaus-Jürgen, and Bouzinov, Pavel A. “A finite element procedure for the analysis of thermo-mechanical solids in contact”. In: *Computers & Structures* 75.6 (2000), pp. 551–573. ISSN: 0045-7949. DOI: https://doi.org/10.1016/S0045-7949(99)00212-6. URL: https://www.sciencedirect.com/science/article/pii/S0045794999002126.

[60] Liang, Xiaodong, Ali, Mohammad Zawad, and Zhang, Huaguang. “Induction Motors Fault Diagnosis Using Finite Element Method: A Review”. In: *IEEE Transactions on Industry Applications* 56.2 (2020), pp. 1205–1217. DOI: 10.1109/TIA.2019.2958908.

[61] Ye, Zhiqiu et al. "Soft Robot Skin With Conformal Adaptability for On-Body Tactile Perception of Collaborative Robots". In: *IEEE Robotics and Automation Letters* (Mar. 2022), pp. 1–1. doi: 10.1109/LRA.2022.3155225.

[62] Lu, Guan, Fu, Shiwen, and Xu, Yiming. "Design and Experimental Research of Robot Finger Sliding Tactile Sensor Based on FBG". In: *Sensors* 22.21 (2022). issn: 1424-8220. doi: 10.3390/s22218390. url: https://www.mdpi.com/1424-8220/22/21/8390.

[63] Ciocarlie, M., Miller, A., and Allen, P. "Grasp analysis using deformable fingers". In: *2005 IEEE/RSJ International Conference on Intelligent Robots and Systems*. 2005, pp. 4122–4128. doi: 10.1109/IROS.2005.1545525.

[64] Narang, Yashraj S. et al. "Sim-to-Real for Robotic Tactile Sensing via Physics-Based Simulation and Learned Latent Projections". In: *CoRR* abs/2103.16747 (2021). arXiv: 2103.16747. url: https://arxiv.org/abs/2103.16747.

[65] Narang, Yashraj S. et al. "Interpreting and Predicting Tactile Signals via a Physics-Based and Data-Driven Framework". In: *CoRR* abs/2006.03777 (2020). arXiv: 2006.03777. url: https://arxiv.org/abs/2006.03777.

[66] Sferrazza, Carmelo et al. "Ground Truth Force Distribution for Learning-Based Tactile Sensing: A Finite Element Approach". In: *IEEE Access* PP (Nov. 2019), pp. 1–1. doi: 10.1109/ACCESS.2019.2956882.

[67] Calandra, Roberto et al. "More Than a Feeling: Learning to Grasp and Regrasp using Vision and Touch". In: *CoRR* abs/1805.11085 (2018). arXiv: 1805.11085. url: http://arxiv.org/abs/1805.11085.

[68] Spiers, Adam et al. "Single-Grasp Object Classification and Feature Extraction with Simple Robot Hands and Tactile Sensors". In: *IEEE Transactions on Haptics* 9 (Jan. 2016), pp. 60–71. doi: 10.1109/TOH.2016.2521378.

[69] Higuera, Carolina, Boots, Byron, and Mukadam, Mustafa. *Learning to Read Braille: Bridging the Tactile Reality Gap with Diffusion Models*. 2023. arXiv: 2304.01182 [cs.RO].

[70] Ruppel, Philipp et al. "Simulation of the SynTouch BioTac Sensor". In: (2019). Ed. by Strand, Marcus et al., pp. 374–387.

[71] Huang, Xiaoshui et al. *A comprehensive survey on point cloud registration*. 2021. arXiv: 2103.02690 [cs.CV].

[72] Oberweger, Markus, Wohlhart, Paul, and Lepetit, Vincent. *Hands Deep in Deep Learning for Hand Pose Estimation*. 2016. arXiv: 1502.06807 [cs.CV].

[73] Toshev, Alexander and Szegedy, Christian. "DeepPose: Human Pose Estimation via Deep Neural Networks". In: *Computer Vision and Pattern Recognition*. 2014.

[74] Mathis, Alexander et al. "DeepLabCut: markerless pose estimation of user-defined body parts with deep learning". In: *Nature Neuroscience* 21.9 (Sept. 2018), pp. 1281–1289. issn: 1546-1726. doi: 10.1038/s41593-018-0209-y. url: https://doi.org/10.1038/s41593-018-0209-y.

[75] Huang, Xiaoshui et al. "A Systematic Approach for Cross-Source Point Cloud Registration by Preserving Macro and Micro Structures". In: *IEEE Transactions on Image Processing* 26.7 (2017), pp. 3261–3276. doi: 10.1109/TIP.2017.2695888.

[76] Huang, Xiaoshui et al. "A Coarse-to-Fine Algorithm for Matching and Registration in 3D Cross-Source Point Clouds". In: *IEEE Transactions on Circuits and Systems for Video Technology* 28.10 (2018), pp. 2965–2977. doi: 10.1109/TCSVT.2017.2730232.

[77] Yang, Zhenpei et al. "Extreme Relative Pose Estimation for RGB-D Scans via Scene Completion". In: June 2019, pp. 4526–4535. doi: 10.1109/CVPR.2019.00466.

[78] Wang, Lingjing et al. *Non-Rigid Point Set Registration Networks*. 2019. arXiv: 1904.01428 [cs.GR].

[79] Huang, Xiaoshui, Mei, Guofeng, and Zhang, Jian. *Feature-metric Registration: A Fast Semi-supervised Approach for Robust Point Cloud Registration without Correspondences*. 2020. arXiv: 2005.01014 [cs.CV].

[80] Zeng, Andy et al. *3DMatch: Learning Local Geometric Descriptors from RGB-D Reconstructions*. 2017. arXiv: 1603.08182 [cs.CV].

[81] Deng, Haowen, Birdal, Tolga, and Ilic, Slobodan. *PPFNet: Global Context Aware Local Features for Robust 3D Point Matching*. 2018. arXiv: 1802.02669 [cs.CV].

[82] Gojcic, Zan et al. *The Perfect Match: 3D Point Cloud Matching with Smoothed Densities*. 2019. arXiv: 1811.06879 [cs.CV].

[83] Besl, Paul J. and McKay, Neil D. "A Method for Registration of 3-D Shapes". In: *IEEE Trans. Pattern Anal. Mach. Intell.* 14 (1992), pp. 239–256.

[84] Chen, Yang and Medioni, Gérard. "Object modelling by registration of multiple range images". In: *Image and Vision Computing* 10.3 (1992). Range Image Understanding, pp. 145–155. ISSN: 0262-8856. DOI: https://doi.org/10.1016/0262-8856(92)90066-C. URL: https://www.sciencedirect.com/science/article/pii/026288569290066C.

[85] Segal, Aleksandr, Hähnel, Dirk, and Thrun, Sebastian. "Generalized-ICP". In: June 2009. DOI: 10.15607/RSS.2009.V.021.

[86] Shi, Xiaojing, Liu, Tao, and Han, Xie. "Improved Iterative Closest Point(ICP) 3D point cloud registration algorithm based on point cloud filtering and adaptive fireworks for coarse registration". In: *International Journal of Remote Sensing* 41.8 (2020), pp. 3197–3220. DOI: 10.1080/01431161.2019.1701211. eprint: https://doi.org/10.1080/01431161.2019.1701211. URL: https://doi.org/10.1080/01431161.2019.1701211.

[87] Zhu, Hao et al. "A Review of Point Set Registration: From Pairwise Registration to Groupwise Registration". en. In: *Sensors (Basel)* 19.5 (Mar. 2019).

[88] Livi, Lorenzo and Rizzi, Antonello. "The Graph Matching Problem". In: *Pattern Anal. Appl.* 16.3 (Aug. 2013), pp. 253–283. ISSN: 1433-7541. DOI: 10.1007/s10044-012-0284-8. URL: https://doi.org/10.1007/s10044-012-0284-8.

[89] Zhou, Feng and De la Torre, Fernando. "Factorized Graph Matching". In: *IEEE Transactions on Pattern Analysis and Machine Intelligence* 38.9 (2016), pp. 1774–1789. DOI: 10.1109/TPAMI.2015.2501802.

[90] Leordeanu, Marius and Hebert, Martial. "A spectral technique for correspondence problems using pairwise constraints". In: *Tenth IEEE International Conference on Computer Vision (ICCV'05) Volume 1* 2 (2005), 1482–1489 Vol. 2.

[91] Zass, Ron and Shashua, Amnon. "Probabilistic graph and hypergraph matching". In: *2008 IEEE Conference on Computer Vision and Pattern Recognition*. 2008, pp. 1–8. DOI: 10.1109/CVPR.2008.4587500.

[92] Duchenne, Olivier et al. "A Tensor-Based Algorithm for High-Order Graph Matching". In: *IEEE Transactions on Pattern Analysis and Machine Intelligence* 33.12 (2011), pp. 2383–2395. DOI: 10.1109/TPAMI.2011.110.

[93] Zhu, Hu et al. "Elastic Net Constraint-Based Tensor Model for High-Order Graph Matching". In: *IEEE Transactions on Cybernetics* 51.8 (2021), pp. 4062–4074. DOI: 10.1109/TCYB.2019.2936176.

[94] Müller, Meinard. *Information Retrieval for Music and Motion*. Jan. 2007. ISBN: 978-3-540-74047-6. DOI: 10.1007/978-3-540-74048-3.

[95] Fan, Jingfan et al. “Convex hull indexed Gaussian mixture model (CH-GMM) for 3D point set registration”. In: *Pattern Recognition* 59 (2016). Compositional Models and Structured Learning for Visual Recognition, pp. 126–141. ISSN: 0031-3203. DOI: https://doi.org/10.1016/j.patcog.2016.02.023. URL: https://www.sciencedirect.com/science/article/pii/S0031320316000947.

[96] Evangelidis, Georgios D. et al. “A Generative Model for the Joint Registration of Multiple Point Sets”. In: *Computer Vision – ECCV 2014*. Ed. by Fleet, David et al. Cham: Springer International Publishing, 2014, pp. 109–122. ISBN: 978-3-319-10584-0.

[97] Yuan, Wentao et al. *DeepGMR: Learning Latent Gaussian Mixture Models for Registration*. 2020. arXiv: 2008.09088 [cs.CV].

Appendix A

Appendix A Title